A thermochemical study on the primary oxidation of sulfur

N. Sebbar, J.W. Bozzelli, H. Bockhorn & D. Trimis

A thermochemical study on the primary oxidation of sulfur

N. Sebbar[a], J.W. Bozzelli[b], H. Bockhorn[a], and D. Trimis[a]

[a]KIT- Karlsruhe Institute of Technology, Engler-Bunte-Institut, Combustion Technology, Karlsruhe, Germany; [b]Department of Chemical Engineering, New Jersey Institute of Technology, Newark, New Jersey, USA

ABSTRACT

Several chemical reactions related to the oxidation and combustion of sulfur are investigated using a number of computational chemistry methods with the objective of determining appropriate methods for use in developing an elementary reaction mechanism for oxidation of sulfur. Calculations are focused on thermochemical properties and reaction energetics for reactive species and transition state structures for reactions in the oxidation/combustion of sulfur. Reactions involving several intermediates resulting from the reactions of S_2 with oxygen were investigated with the density functional theory B3LYP (with several basis sets) and BB1K/GTLarge. The composite ab-initio methods G2, G3, G3MP2, G3B3, G3MP2B3 and CBS-QB3 were also used. Enthalpies of a series of sulfur compounds and transition state structures are calculated using the ab-initio and DFT calculations. The calculations were combined with isodesmic reaction analysis, whenever possible, in order to cancel error and improve the accuracy of the calculations. Results show that all B3LYP DFT calculations including the 6–311++G(3df,2p) basis set show poor outcome in estimating the enthalpy of reactions involving S_2. The six composite methods have all shown consistency with each other and their calculated reaction energies/bond energies are in good agreement with the available literature. Kinetic parameters for calculation of the kinetic parameters on SO_3 dissociation to SO_2 and O using the canonical transition state theory are reported.

1. Introduction

Combustion of elemental sulfur is performed in large scale as a part of the industrial production process of sulfuric acid which is one of the world's largest volume industrial chemicals. As such, sulfur combustion in existing facilities is technically robust and mostly designed to realize large product streams (Louie, 2005; PEGASUS, 2016). Electricity generation may be carried out with the heat generated from sulfur combustion and the process is independent of encasement: Sulfur is a very cost-effective material and can be inexpensively stored outdoor under ambient conditions for long times and in large quantities (PEGASUS, 2016). In contrast, there has been relatively little research on the combustion of elemental sulfur.

Several studies have focused on the oxidation of SO_2 to SO_3. Naidoo et al. (2005) have conducted an experimental kinetic study of the SO_2 + O association and Jiang et al. (2009) have reported a quantum chemistry study on the reaction of SO_2 with O_3 and H_2O_2. The reactions of diatomic sulfur S_2 in the atmosphere with O, O_2 and O_3 and HO_2 have been investigated in the experimental work of Hills et al. (1987) and rates of some reactions have been determined. Little data on the kinetics of SO_3 dissociation and sulfur combustion are available. Yilmaz et al. (2006) have conducted experiments on the thermal dissociation of SO_3 in the temperature range of 1000–1400 K and have determined a rate constant for $SO_3 + N_2 \rightarrow SO_2 + O + N_2$.

The main purpose of the present work is to compile, test and validate the performance of one or several computational methods to provide accurate results for the thermochemical properties of reactions and rate coefficients of the combustion of elemental sulfur. A further goal is to develop a detailed reaction mechanism for the reactions of the $S_2 + O_2$ system on the basis of elementary reactions. We compare also quantum chemistry-based calculations with the experimental values of Yilmaz et al. (2006).

2. Computational methods

Thermochemical and kinetic properties for sulfur compounds (stable molecules, radicals and transition state structures) are calculated with the help of several computational methods using the Gaussian 03 program suite (Gaussian 03, Revision A.1. et al. 2003). Hybrid density functional theory (DFT) methods are used with B3LYP/6+311G(d,p), B3LYP/6–311+G(d,p), B3LYP/6–311+G(2d, p), B3LYP/6–311++G(3df, 2p), B3LYP/CBSB7 (Baboul et al., 1999; Becke, 1992a, 1992b, 1993; Redfern et al., 2000) basis sets. The hybrid Hartree–Fock-density functional model called the Becke88-Becke95 1-parameter model for kinetics BB1K/GTLarge (Montgomery et al., 1994; Zhao et al., 2004) is also evaluated. Six composite methods (ab-initio) are tested and used in this work. G2 (Curtiss et al., 1991), G3 (Curtis et al., 1998), G3 theory performs a sequence of ab-initio molecular orbital calculations selected to remove errors and further calibrated to yield an accurate total energy for a species. Optimized structures and frequencies are obtained at the Hartree–Fock HF/6-31G(d) level and G3MP2 (Curtiss et al., 1999). The modified G3 theory using B3LYP geometries was employed and referred as G3MP2B3 (Baboul et al., 1999; Redfern et al., 2000) and G3B3. These last two methods use geometries and zero-point energies at the B3LYP/6-31G(d) level. Finally, the well-regarded CBS-QB3 (Montgomery et al., 1999) is also examined for use in the sulfur/oxygen system.

3. Results and discussion

3.1. *Validation of methods with known enthalpy values for sulfur compound*

3.1.1. *Enthalpy of formation*

Geometries and standard enthalpies of formation of some reactants, products and transition state structures describing the primary reactions for the combustion of sulfur are reported. In order to find accurate computational methods, DFT methods at several levels and composite ab-initio methods are used. Standard enthalpies are calculated using different isodesmic reactions (hypothetical reactions with similarity in mass and bonding environments for reactant and product sets in order to provide cancellation of systematic errors). Transition state structure (TS) enthalpies were obtained from the computational energy of the TS structure relative to both the reactants and products. Zero-point energies

(ZPVEs) and thermal corrections to 298.15 K are applied for all calculations. Frequencies and moments of inertia are obtained from each method in order to calculate the entropies and heat capacities. The latter results are not reported in this study.

Tables 1 and 2 list the calculated enthalpy of formation (kcal mol ^{1}) for SO, SO_2, SO_3 and SSO along with literature values for comparison. Table 1 reports the calculated values from six composite ab-initio methods (CBS-QB3, G2, G3, G3MP2, G3B3 and G3MP2B3), while in Table 2, a series of DFT calculations at six levels (B3LYP at different basis sets and BB1K) are listed. The enthalpies, $\Delta_f H^0_{298}$, listed in Table 1 show very good agreement with the literature values and precision through the different work reactions.

The spin value (singlet, triplet) is of crucial importance in the calculation of the energy and consequently in the determination of the thermodynamics and kinetics. We note a deviation of 1 to 4 kcal mol ^{1} among the composite methods and the literature values. All of the DFT calculations gave poor outcome for the calculation of enthalpies of these sulfur species at all basis levels, while the calculation of the structure parameters (lengths, angles, dihedrals) is in good agreement with literature data (Durant, 1996; Andino et al., 1996; Curtiss et al., 2000; Petersson et al., 1998; Wong and Radom, 1998; Mayer et al., 1998; Sebbar et al., 2005a, 2005b). It appears that, for oxygenated sulfur compounds, DFT is not eligible. Therefore, for further investigations in developing an elementary reaction mechanism for oxidation of sulfur, the six composite methods are selected and will be used.

3.1.2. *Bond energy calculations*

The dissociation reaction of SO_3 to SO_2 + O assimilated to S—O bond energy (BE) in the SO_3 molecule has been determined at different levels of calculation (DFT and ab-initio). For each method, the bond energy is estimated as the calculated energy difference between the products and adducts and converted into kcal mol ^{1}. The BE values are listed in Table 3. According to reported enthalpies in the literature (NIST), the S—O bond energy is calculated to be 83.20 kcal mol ^{1}. The different B3LYP methods listed in Table 3 yield lower BE values (62–75 kcal mol ^{1}) while all six composite methods calculations (G2, G3, G3MP2, G3B3, G3MP2B3 and CBS-QB3) are near 81–83 kcal mol ^{1} which is in very good agreement with the literature. We note a deviation of only 0.4 and 1.1 kcal mol ^{1} between CBS-QB3 and G2 value from literature.

The S—O bond energy (BE) in the SO_2 molecule has been also determined at different levels of calculation (DFT and ab-initio) and is listed in Table 4. Based on enthalpies reported in the literature (NIST), the S—O bond energy in SO_2 is calculated to be strong with 130.14 kcal mol ^{1}. As above, all B3LYP methods yield lower BE values (103–120 kcal mol ^{1}) while all six composite methods calculations are very similar by 130–138 kcal mol ^{1}. We note a difference of less than 1 kcal mol ^{1} between CBS-QB3, G3B3, G3MP2B3 and literature.

The third molecule tested for the validation of the methods is SSO, with two different bonds, S—O (at 102.24 kcal mol ^{1}) and S—S (at 80.95 kcal mol ^{1}). The S—O bond is stronger by some 22 kcal mol ^{1} than S—S. We also note that S—O (in SSO) is stronger by 19 kcal mol ^{1} than in SO_3 but weaker by 28 kcal mol ^{1} than in SO_2. The calculated S—S and S—O BE using the same methods and listed in Table 5 confirm the above observations, namely that DFT is not eligible for oxygenated sulfur compounds.

Table 1. Enthalpy of formation for species resulting from several sulfur/oxygen systems calculated at CBS-QB3, G2, G3, G3B3, G3MP2 and G3MP2B3 levels (in kcal mol^{-1}).

Structure	Reactions	$\Delta_f H^0_{298}$ in kcal mol^{-1}					
		CBS-QB3	G2	G3	G3B3	G3MP2	G3MP2B3
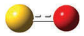	SO → ^{3}S + ^{3}O	**−1.23**	**1.86**	**0.44**	**0.20**	**1.02**	**0.47**
	NIST = 1.2						
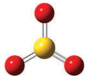	SO$_2$ + ^{3}O → SO$_3$	−94.22	−93.45	−93.12	−92.61	−92.02	−91.72
	SO$_3$ → SO + ^{3}O$_2$	−92.53	−96.33	−91.06	−90.39	−91.32	−90.28
	SO$_3$ → ^{3}S + ^{3}O + ^{3}O$_2$	−93.41	−94.11	−90.27	−89.84	−89.95	−89.46
	^{3}S$_2$ + 3^{3}O$_2$ → 2SO$_3$	−92.40	−96.10	−91.53	−90.60	−90.97	−89.61
	NIST = −94.59	**−93.14 ± 0.8**	**−95.00 ± 1.4**	**−91.50 ± 1.2**	**−90.86 ± 1.2**	**−91.07 ± 0.9**	**−90.27 ± 1.0**
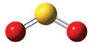	2^{3}SO + ^{3}O$_2$ → 2SO$_2$	−69.55	−72.66	−68.20	−68.64	−69.11	−69.17
	S^3 + O2^3 → SO2	−70.13	−71.60	−68.09	−68.17	−68.87	−68.68
	^{3}S$_2$ + 2^{3}O$_2$ → 2SO$_2$	−69.42	−72.44	−68.67	−68.86	−68.76	−68.50
	NIST = −70.939	**−69.70 ± 0.4**	**−72.23 ± 0.6**	**−68.32 ± 0.3**	**−68.56 ± 0.3**	**−68.91 ± 0.2**	**−68.78 ± 0.3**
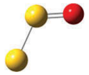	^{3}SSO → ^{3}O + ^{3}S$_2$	−13.17	−15.72	−12.16	−12.86	−12.15	−12.79
	^{3}SSO → ^{3}S + ^{3}SO	−12.16	−14.72	−10.23	−10.49	−12.19	−12.42
	NIST = −13.50	**−12.67 ± 0.7**	**−15.22 ± 0.5**	**−11.19 ± 0.9**	**−11.68 ± 1.2**	**−12.17 ± 0.02**	**−12.60 ± 0.2**

Table 2. Enthalpy of formation for species resulting from several sulfur/oxygen systems with the DFT methods, B3LYP and BB1K and indicated basis sets (in kcal mol ^{1}).

		$\Delta_f H^0_{298}$ in kcal mol^{-1}					
Structure	Reactions	B3LYP/6 311G(d,p)	B3LYP/6 311 + G(d,p)	B3LYP/6 311 + G(2d.p)	B3LYP/6 311 ++G (3df,2p)	B3LYP/ CBSB7	BB1K/ GTlarge
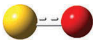	$^3SO \rightarrow {}^3S + {}^3O$ NIST = 1.2	**12.96**	**11.32**	**4.90**	**0.13**	**8.08**	**7.21**
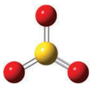	$SO_2 + {}^3O \rightarrow SO_3$	73.46	70.33	79.57	87.27	81.39	85.03
	$SO_3 \rightarrow SO + {}^3O_2$	75.10	71.73	89.71	74.29	91.96	81.35
	$SO_3 \rightarrow {}^3S + {}^3O + {}^3O_2$	32.76	31.72	55.96	73.81	54.50	61.86
	$^3S_2 + 3^3O_2 \rightarrow 2SO_3$	38.78	37.71	57.87	73.17	56.77	49.70
	NIST = 94.59	**55.03**	**52.88**	**70.78**	**77.13**	**71.15**	**69.48**
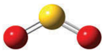	$2SO_3 + {}^3O_2 \rightarrow 2SO_2$	43.00	42.41	52.22	58.56	51.93	50.11
	$^3S + {}^3O_2 \rightarrow SO_2$	30.24	32.33	47.33	57.48	44.05	47.77
	$S2^3 + 2O2^3 \rightarrow 2SO2$	35.71	36.73	48.88	57.44	45.77	44.81
	NIST = 70.939	**36.32**	**37.16**	**49.48**	**57.83**	**47.25**	**47.56**
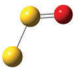	$^3SSO \rightarrow {}^3O + {}^3S_2$	11.29	12.07	21.50	4.53	18.72	30.48
	$^3SSO \rightarrow {}^3S + SO$	18.54	19.02	27.88	3.54	28.55	33.27
	NIST = 13.50	**14.91**	**15.54**	**24.69**	**4.04**	**23.64**	**31.87**

Table 3. S—O Bond energy in SO_3 in kcal mol ^{1}.

$SO_3 \rightarrow SO_2 + O$ *Literature* = 83.20 (NIST)			
Method basis set	BE (kcal mol^{-1})	Method basis set	BE (kcal mol^{-1})
B3LYP/6 311G(d,p)	62.07	CBS QB3	82.83
B3LYP/6 311 + G(d,p)	58.94	G2	82.06
B3LYP/6 311G+(2d,p)	68.18	G3	81.73
B3LYP/6 311G++(3df,2p)	75.88	G3B3	81.22
B3LYP/CBSB7	70.0	G3MP2	80.63
BB1K	73.64	G3MP2B3	80.34

Table 4. S—O Bond energy in SO_2 in kcal mol ^{1}.

$SO_2 \rightarrow SO + O$ *Literature* = 130.14 (NIST)			
Method basis set	BE (kcal mol^{-1})	Method basis set	BE (kcal mol^{-1})
B3LYP/6 311G(d,p)	103.2	CBS QB3	130.61
B3LYP/6 311 + G(d,p)	101.57	G2	132.26
B3LYP/6 311G+(2d,p)	112.61	G3	128.28
B3LYP/6 311G++(3df,2p)	119.9	G3B3	129.32
B3LYP/CBSB7	112.13	G3MP2	138.73
BB1K	120.06	G3MP2B3	129.59

Table 5. S—O and S—S bond energies in SSO in kcal mol ^{1}.

$^3SSO \rightarrow {}^2SS + {}^3O/{}^3SSO \rightarrow {}^3S + {}^3SO$ *Literature* = 102.24/80.95 (NIST)					
	BE (kcal mol^{-1})			BE (kcal mol^{-1})	
Method basis set	S O	S S	Method basis set	S O	S S
B3LYP/6 311G(d,p)	77.43	56.95	CBS QB3	101.91	79.61
B3LYP/6 311 + G(d,p)	78.09	58.12	G2	104.46	82.16
B3LYP/6 311G+(2d,p)	87.52	66.83	G3	100.89	77.67
B3LYP/6 311G++(3df,2p)	93.27	70.99	G3B3	101.6	77.93
B3LYP/CBSB7	84.82	66.97	G3MP2	100.88	79.63
BB1K	98.15	74.76	G3MP2B3	101.52	79.86

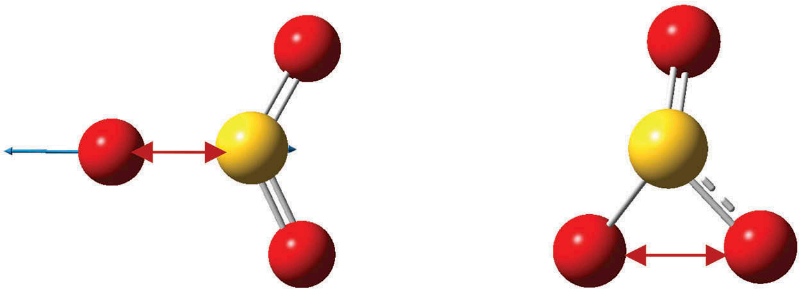

Figure 1. Left: Structure of TS-SO_3-A at CBS-QB3, G2, G3 and G3MP2. Right: Structure of TS-SO_3-B at CBS-QB3, G3B3 and G3MP2B3.

3.2. *Calculations for other species involved in sulfur oxidation*

3.2.1. *Enthalpy of formation of stable species and enthalpies of transition state structures*

Table 6 illustrates structures and lists the calculated standard enthalpies of formation of four species. All calculated enthalpies show very good agreement throughout the six composite methods. A second structure for SO_3 (Table 6) has been observed. The structure is non planar, one S=O double bond can be seen at 1.47 Å and two S—O single bonds at 1.63 Å. This structure is stable but the corresponding enthalpy is significantly higher with 64 kcal mol ^{1} at −30.71 kcal mol ^{1} (at CBS-QB3 level). This structure might come into play in building of a reaction mechanism.

There are also two calculated geometries for SSO, one structure is bent as illustrated in Table 1 and one is linear as illustrated in Table 6. The calculated enthalpy of the linear form of SSO is much higher with 26.77 kcal mol ^{1} versus −12.67 kcal mol ^{1} for the bent form (both at CBS-QB3 level). This higher energy geometry is not used in the present work but should be also considered in the elaboration of a mechanism. A new stable species, SS(=O)=O, with consistent enthalpy value among the different methods is calculated and reported in Table 6.

Table 7 illustrates seven transition state structures determined at the six composite levels. Transition state structures have been identified for both SO_3 geometries. The TSO_3-A structure results from the planer SO_3 and clearly shows one oxygen atom leaving the SO_3 molecule, as illustrated in Figure 1 (left). This structure also shows two S=O double bonds, while the third S—O at 2.02 Å has the oxygen leaving the sulfur atom. The calculated enthalpy values for this TSO_3-A are in agreement with each other.

The transition state structure of the non-planar SO_3 (TSO_3-B) is illustrated in Figure 1 (right). The vibrations show oxygens 2 and 3 moving to form a new O—O bond and SO plus O_2. This structure has been obtained with the CBS-QB3, G3B3 and G3MP2B3 methods at enthalpy values of −8.39, −3.76 and −3.31 kcal mol ^{1}, respectively. The three other methods (G2, G3, G3MP2) appear to convert the molecule to the TSO_3-A structure and suggest that only B3LYP geometries calculations (if this study) identify TSO_3-B. Another interpretation of this TSO_3-B transition structure is that the non-planar SO_3, which is at −31 kcal mol ^{1}, tries to flatten to reach the planer geometry at a lower energy

Table 6. Enthalpy of formation for species resulting from several sulfur/oxygen systems calculated at CBS-QB3, G2, G3, G3B3, G3MP2 and G3MP2B3 levels (in kcal mol^{-1}).

		$\Delta_f H^0_{298}$ in kcal mol^{-1}					
Structure	Reactions	CBS-QB3	G2	G3	G3B3	G3MP2	G3MP2B3
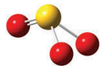	$SO_2 + {}^3O \rightarrow SO_3$	−31.79	−32.33	−31.24	−30.32	−30.57	−29.89
	$SO_3 \rightarrow {}^3SO + {}^3O_2$	−30.10	−35.21	−29.18	−28.09	−29.87	−28.45
	$SO_3 \rightarrow {}^3S + O^3 + {}^3O_2$	−30.98	−32.99	−28.39	−27.55	−28.50	−27.63
	$2SO_3 \rightarrow {}^3S_2 + 3{}^3O_2$	−29.97	−34.98	−29.66	−28.31	−29.52	−27.78
	Average	**−30.71 ± 0.8**	**−33.88 ± 1.4**	**−29.62 ± 1.2**	**−28.57 ± 1.2**	**−29.62 ± 0.9**	**−28.44 ± 1.0**
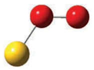	$SOO \rightarrow {}^3O_2 + {}^3S$	47.54	42.80	46.25	47.42	46.76	47.78
	$SOO \rightarrow {}^3SO + {}^3O$	46.27	41.35	45.26	45.47	46.10	46.07
	Average	**46.90 ± 0.9**	**42.08 ± 1.0**	**45.76 ± 0.7**	**46.44 ± 1.38**	**46.43 ± 0.5**	**46.92 ± 1.2**
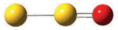	${}^3SSO\text{-}L \rightarrow {}^3O + {}^3S2$	26.26	25.66	26.46	26.36	26.96	26.09
	${}^3SSO\text{-}L \rightarrow {}^3S + {}^3SO$	27.27	26.66	28.39	28.73	26.92	26.46
	Average	**26.77 ± 0.7**	**26.16 ± 0.7**	**27.43 ± 1.4**	**27.55 ± 1.68**	**26.94 ± 0.03**	**26.27 ± 0.3**
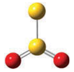	$SS(=O)=O \rightarrow SO_2 + S^3$	−42.39	−41.59	−41.22	−40.10	−41.39	−40.60
	$SS(=O)=O \rightarrow SSO + O^3$	−44.19	−42.50	−42.63	−42.29	−41.29	−41.14
	Average	**−43.29 ± 1.3**	**−42.05 ± 0.6**	**−41.92 ± 1.0**	**−41.20 ± 1.5**	**−41.34 ± 0.1**	**−40.87 ± 0.4**

Table 7. Enthalpies for transition state structures from sulfur/oxygen systems calculated at CBS-QB3, G2, G3, G3B3, G3MP2 and G3MP2B3 levels (in kcal mol^{-1}). The listed two values give the enthalpies of the TS structures calculated relative to both the reactants and products.

Structure	Reactions	LMin kcal mol^{-1}					
		CBS-QB3	G2	G3	G3B3	G3MP2	G3MP2B3
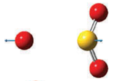	$SO_2 + {}^3O \rightarrow TSO_3$-A	−17.37	−11.58	−14.77		−14.09	
	TSO_3-A → SO_3	−16.19	−11.17	−14.69	Fails	−15.11	Fails
	Average	**−16.78 ± 0.8**	**−11.38 ± 0.3**	**−14.73 ± 0.06**		**−14.60 ± 0.7**	
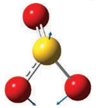	$SO_2 + {}^3O \rightarrow TSO_3$-B	−7.80			−3.98		−3.97
	TSO_3-B → SO_3	−8.98	Fails	Fails	−3.54	Fails	−2.65
	Average	**−8.39 ± 0.8**			**−3.76 ± 0.3**		**−3.31 ± 0.9**
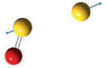	SSO → TOS-S	65.60				61.79	62.17
	TOS-S → ${}^3S + {}^3SO$	66.94				63.10	63.26
	Average	**66.27 ± 0.9**				**62.45 ± 0.9**	**62.71 ± 0.8**
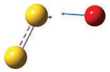	SSO → TSS-O		83.71	80.20		88.55	
	TSS-O → ${}^3S_2 + {}^3O$	Fails	81.49	81.55	Fails	89.90	Fails
	Average		**82.60 ± 1.6**	**80.88 ± 0.9**		**89.90 ± 0.9**	
	SO + O → TSOO	138.56			119.82		130.53
	TSOO → SOO	137.92			118.85		129.67
	Average	**138.24 ± 0.4**			**119.34 ± 0.7**		**130.10 ± 0.6**
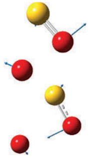	SOO → TSO_2	120.04	126.10	127.90	116.71	128.05	117.88
	$TSO_2 \rightarrow SO_2$	119.87	127.49	125.55	114.92	126.31	116.47
	Average	**119.96 ± 0.1**	**126.79 ± 1.0**	**126.73 ± 1.7**	**115.81 ± 1.3**	**127.18 ± 1.2**	**117.17 ± 1.0**
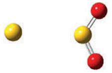	SS(=O)(=O) → TS	20.77	22.05	20.68	19.93	21.90	21.08
	TS → $SO_2 + {}^3O$	21.68	22.51	21.39	21.03	21.85	21.35
	Average	**21.23 ± 0.6**	**22.28 ± 0.3**	**21.03 ± 0.5**	**20.48 ± 0.8**	**21.87 ± 0.04**	**21.21 ± 0.2**

of −94 kcal mol ^{1}. This possible reaction needs to be carefully investigated in a future work.

SSO (S_2O) can undergo dissociation by splitting the S—O or the S—S bonds. These dissociations are, however, high energetic and difficult to find with all methods. Only the G3MP2 level could find the cleavage of the S—S bond clearly. CBS-QB3 and G3MP2B3 showed a sort of "umbrella" transition state. Despite the different transition state structure, CBS-QB3 and G3MP2B3 enthalpy values are in agreement with that of G3MP2 structure. The O—O in SSO needs higher energy to cleave than the S—O. For these reactions, only the MP2 calculations could "identify" a transition state structure, namely G2, G3 and G3MP2. In some cases, calculations with MP2 make sequential reactions as observed in a previous work (Sebbar et al., 2014).

An interesting transition state (TSOO) resulting from the SO + O association was identified with the six methods. The resulting enthalpy value for these structures varies within the methods. The methods using B3LYP for the optimization of geometries, CBS-QB3, G3B3 and G3MP2B3 have calculated imaginary frequency of −943.4, −908.3 and −908.3 cm ^{1}, respectively. The three other composite methods, G2, G3 and G3MP2B3, estimated the imaginary frequency at −1026.66 cm ^{1}. Comparison of the O—O and S—O distances in these two set of methods show that all O—O and S—O distances are shorter than those from methods involving MP2 calculations. Similar results are obtained with the TSO_2 transition state structure. The group CBS-QB3, G3B3 and G3MP2B3 methods calculated an imaginary frequency at −827.4, −861.9 and −861.9 respectively, versus −270.5 for the group G2, G3 and G3MP2. The O—O distance with the first set of methods is significantly shorter with 1.94 Å versus 2.46 Å. The enthalpy value for this transition state is likely to be about 116–119 kcal mol ^{1}.

3.3. *Reaction of SO_2 + O^{3p} to SO_3: Potential diagram and kinetics*

3.3.1. *Potentials for SO_2 + O^{3p} → SO_3*

Figure 2, illustrates the formation of SO_3 from SO_2 + ^3O association. On the left, we can see that the more stable planar form of SO_3 is highly exothermic with some 80 kcal mol ^{1} and the association occurs without barrier. On the right side of Figure 2, formation of the

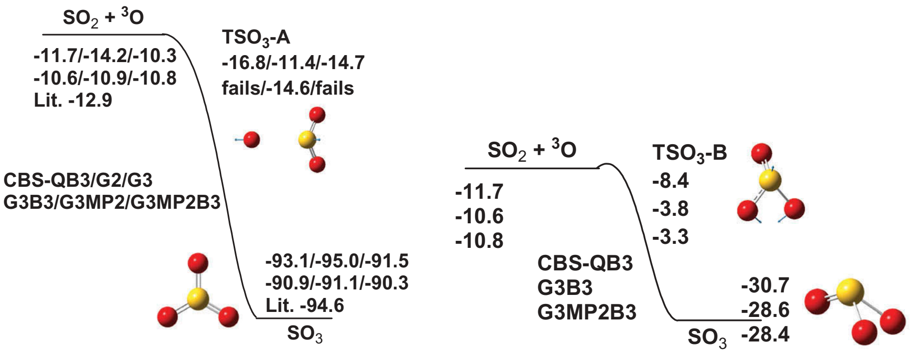

Figure 2. Left: Structure of TS-SO_3-A at CBS-QB3, G2, G3 and G3MP2. Right: Structure of TS-SO_3-B at CBS-QB3, G3B3 and G3MP2B3.

non-planar SO_3 is also exothermic, but to a much lower extend with some 20 kcal mol ^{1}. For this SO_3-B transition state structure a small barrier is required.

3.3.2. *Kinetic calculations for $SO_3 \rightarrow SO_2 + O^{3p}$*

The reaction of SO_3 to SO_2 can also occur under catalytic conditions (Yilmaz et al., 2006). The decomposition of SO_3 is a slow but important reaction and can serve to control the O_2 concentration in the SO_3-H_2O decomposition system (Zhang et al., 2014). The kinetic parameters for the dissociation of the two structures of SO_3 have been evaluated with the results of the composite methods.

The reaction rate constants for this unimolecular dissociation reaction have been calculated on the basis of the canonical transition state theory (IUPAC, 2006) and are listed in Table 8 along with the results of Yilmaz et al. (2006) and Zhang et al. (2014). Good agreement can be seen within the composite methods. The activation energy for TS-SO3 planar (TSO3-A) is close to that determined by Zhang et al. (2014). The structure TS-SO3-B results in a lower activation energy.

We have also compared the effect of the standard deviation of enthalpy on the kinetic parameters. The enthalpy of TS-SO3-A calculated with CBS-QB3 is −16.78 ± 0.83, resulting in the following parameters variation: The re-exponential factor A varies from 4.51E+13 to 3.42E+13 which is about 25% and the activation energy varies by 1% which is not significant. On the other hand, G3 calculation shows that the pre-exponential factor A is not affected by the standard deviation of the enthalpy (−14.73 ± 0.06) and Ea deviates by less than 1%. However, these observations don't imply that G3 is more accurate for identifying transition state structures. According to literature, CBS methods have higher accuracy because they approximate an infinitely large basis set by combining energies from many lower-level theories and the geometries calculations are based on B3LYP. For MP2-based methods like G3, it is more difficult to find transition state structures but on the other hand MP2 can see a structure which is not stable when using B3LYP geometries optimization. Our point of view is that first, experimental data would be of big help to determine the right kinetic parameters and second, different level of calculations are still needed to determine the kinetic of a reaction. The low activation energies from the experiments in the literature compared with the calculated ones indicate that the reactions could be more complex and consist of sequential reactions.

Table 8. Kinetic parameters for the reaction $SO_3 \rightarrow SO_2 + O$ in CHEMKIN format.

k = A T^n b exp (E/RT)			
AT^n (cm^3 mol^{-1} sec^{-1}), Ea (cal mol^{-1})			
Methods	A	n	Ea
Kinetic parameters for TS SO3 A Planar			
CBS QB3	4.5143E+13	0.655	76738
G2	5.9034E+10	1.343	83960
G3	1.0020E+12	0.841	77062
G3MP2	1.0020E+12	0.841	76762
Kinetic parameters for TS SO3 B non planar			
CBS QB3	1.0216E+12	0.337	22766
G3B3	3.7368E+12	0.156	25370
G3MP2B3	5.6091E+12	0.156	25690
Kinetic parameters from literature			
Yilmaz et al. (2006)	5.70E+17		79480
Zhang et al. (2014)	3.16E+15		63390

3.4. *Reactions of SSO and SO_2*

3.4.1. *Potentials for $^3SSO \rightarrow {}^3S_2 + {}^3O$ and $SSO \rightarrow {}^3SO + {}^3S$*

Reaction enthalpies of SSO relative to the transition state structures TSS-O and TSO-S have been calculated at different levels as listed in Table 7. As illustrated in Figure 3, the oxygen atom cleavage is endothermic by approximately 100 kcal mol ^{1} but the oxygen atom leaves without a significant added barrier. This is similar to reactions of oxygenated hydrocarbons (Sebbar et al., 2005a). The transition state structure for the dissociation of the sulfur atom from SSO is also difficult to identify. At G3MP2 level, the transitions state structure needs near 76 kcal mol ^{1}, relative to SSO, and a barrier of near 13 kcal mol ^{1,} relative to the set of products SO + S, can be seen.

3.4.2. *Potentials for $^3S_2 + {}^3O_2 \rightarrow SS(O=)=O \rightarrow SO_2 + {}^3S$*

There are several reaction paths for the formation of SO_2 reported in the literature (Naidoo et al. 2005; Fleig et al., 2013; Glarborg et al., 1996; Guo et al., 2014; Lu et al., 2004; Merryman and Levy, 1967; Tsuchiya et al., 1997). In the present work we report two new paths calculated at the CBS-QB3 level. The first one (TS1 in Figure 4) is obtained from the association of $^3S_2$ + $^3O_2$. In TS1, an oxygen is bonded to one sulfur atom, forming SSOO expected to occur without barrier. The exact structure of the SSOO needs to be thoroughly investigated and requires new calculations in a future study. TS1 illustrated in Figure 4 shows the intramolecular abstraction of the peroxy oxygen atom to the middle sulfur atom and form a stable SS(=O)=O at −43 kcal mol ^{1} (see Figure 4). CBS-QB3 calculations show clearly the displacement of the oxygen toward the sulfur atom. The subsequent reaction of the new formed molecule (SS(=O)=O) reacts further by cleaving one sulfur atom to form SO_2 and S over about 65 kcal mol ^{1} energy barrier. This reaction is possible looking at the S—S bond energy in SS(=O)=O of 38.6 kcal mol ^{1} which is weak compared with the S—S bond in S_2 of 102 kcal mol ^{1}. It is important to point out that the $^3S_2$ + $^3O_2$, which is a complicated association, leads to the formation of different products and undergoes different transition state structures depending on the structure of the intermediate S_2O_2 formed. This investigation will be reported in a future work.

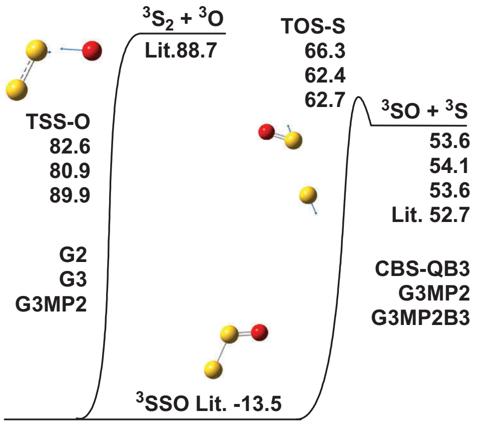

Figure 3. Dissociation of SSO to S_2 + O and SO + S.

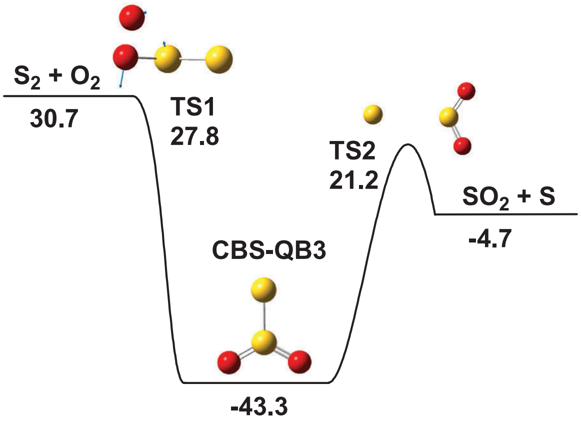

Figure 4. Formation of SO_2 from $S_2 + O_2$ association.

3.4.3. *Potentials for $^3SO + {}^3O \rightarrow SOO \rightarrow SO_2$*

The association of ^{3}SO + O has shown an interesting transition state structure (see Figure 5 and Table 7) calculated with the six composite methods. TS1 in Figure 5 shows clearly the migration of one triplet oxygen atom towards the SO molecule over 62 kcal mol^{-1} (at G3B3 level) relative to the entrance channel and form SOO at lower energy.

The six composite calculations have shown that the most favourable structure is bending the SOO moiety as illustrated in Figure 5 and listed in Table 6. Without consideration of the barrier, only a little overall energy (12 kcal mol^{-1}) is released during formation of the SOO. The SOO$^{\#}$ formed at TS1, however has sufficient energy to pass over TS2 to form the more stable SO_2 by undergoing an intramolecular rearrangement.

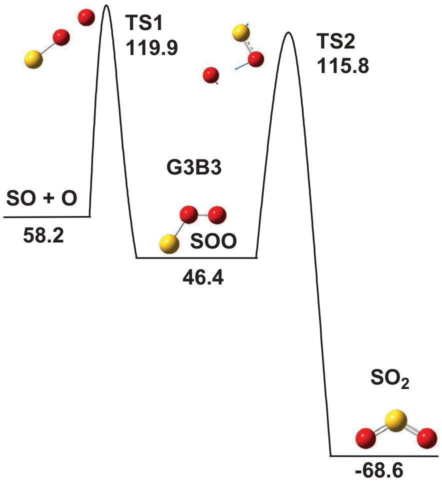

Figure 5. Formation of SO_2 from SO + O association.

Table 9. Standard enthalpies used in this work.

Literature standard enthalpy in kcal mol^{-1}	
S_2	30.736 ± 0.072 (Cox et al. (1984)
SO_2	70.939 ± 0.048 (Chase, 1998)
SO_3	94.591 (Chase, 1998)
SO	1.20 (Chase, 1998)
S	66.245 ± 0.036 (Chase, 1998)
SSO	13.50 (Chase, 1998)

The terminal oxygen undergoes an intramolecular abstraction (TS2 in Figure 5) and shifts to the sulfur atom to form the low energy SO_2 at about −69 kcal mol ^{1}. This isomerization was found to have a barrier of 70 kcal mol ^{1} (at G3B3 level) relative to SOO.

Table 9 reports the known literature values for sulfur compounds for use in the isodesmic reactions and for comparison with own calculations.

4. Conclusions

One objective of this work is to find an appropriate computational method for use in calculating of reaction parameters needed to develop a reaction mechanism for the oxidation of S_2. A series of B3LYP DFT calculations with the basis sets 6–311G(d,p), 6–311+G(d,p), 6-311+G(2d,p), 6-311++G(3df,2p), CBSB7 as well as BB1K/GTLarge brought about poor results in predicting the thermochemistry of SO, SO_2, SO_3 and SSO. Results from six composite methods, G2, G3, G3B3, G3MP2, G3MP2B3 and CBS-QB3 gave good agreement with literature data.

The results have shown that DFT with the basis sets used in this study is not eligible for oxygenated sulfur compounds but all composite ab-initio levels used in this work (several using DFT structures) yield reasonably good results. It also appears that CBS-QB3 and G3MP2B3 yield the best results. This needs to be further elaborated by extending the calculations to a larger number of species. Some kinetic data are reported in this work and some new transition state structures have been identified.

Acknowledgments

The results presented in this study have been obtained within the framework of the PEGASUS project. This project has received funding from the European Union's Horizon 2020 research and innovation program under grant agreement No 727540.

Funding

This work was supported by the European Union's Horizon 2020 research and innovation program [727540].

References

Andino, J.M., Smith, J.N., Flagan, R.C., Goddard, W.A., and Seinfield, J.H. 1996. Mechanism of atmospheric photooxidation of aromatics: a theoretical study. *J. Phys. Chem.*, **100**, 10967 10980.

Baboul, A.G., Curtiss, L.A., Redfern, P.C., and Raghavachari, K. 1999. Gaussian 3 theory using density functional geometries and zero point energies. *J. Chem. Phys. A.*, **110**(16), 7650 7657.

Becke, A.D. 1992a. Density functional thermochemistry. I. The effect of the exchange only gradient correction. *J. Chem. Phys.*, **96**(3), 2155 2160.

Becke, A.D. 1992b. Density functional thermochemistry. II. The effect of the Perdew Wang generalized gradient correlation correction. *J. Chem. Phys.*, **97**(12), 9173 9177.

Becke, A.D. 1993. Density functional thermochemistry. III. The role of exact exchange. *J. Chem. Phys.*, **98**(7), 5648 5852.

Chase, M.W., Jr. 1998. *NIST JANAF Themochemical Tables*, *4th*ed. J. *Phys. Chem.* Ref. Data, Monograph 9, NIST, New York, 1 1951.

Cox, J.D., Wagman, D.D., and Medvedev, V.A. 1984. *CODATA Key Values for Thermodynamics*, Hemisphere Publishing Corp., New York, 1.

Curtiss, L.A., Raghavachari, K., Redfern, P.C., and Pople, J.A. 2000. Assessment of Gaussian 3 and density functional theories for a larger experimental test set. *J. Chem. Phys.*, **112**, 7374.

Curtiss, L.A., Raghavachari, K., Redfern, P.C., Rassolov, V., and Pople, J.A. 1998. Gaussian 3 (G3) theory for molecules containing first and second row atoms. *J. Chem. Phys.*, **109**, 7764 7776.

Curtiss, L.A., Raghavachari, K., and Trucks, G.W. 1991. Gaussian 2 theory for molecular energies of first and second row compounds. *Chem. Phys.*, **94**(11), 7221 7230.

Curtiss, L.A., Redfern, P.C., Raghavachari, K., Rassolov, V., and Pople, J.A. 1999. Gaussian 3 theory using reduced Møller Plesset order. *J. Chem. Phys.*, **110**, 4703.

Durant, J.L. 1996. Evaluation of transition state properties by density functional theory. *Chem Phys Lett.*, **256**, 595.

Fleig, D., Alzueta, M.U., Normann, F., Abián, M., Andersson, K., and Johnsson, F. 2013. Measurement and modeling of sulfur trioxide formation in a flow reactor under post flame conditions. *Combustion and Flame.*, **160**, 1142 1151.

Gaussian 03, Revision A.1, Frisch, M.J., Trucks, G.W., Schlegel, H.B., Scuseria, G.E., Robb, M.A., Cheeseman, J.R., Zakrzewski, V.G., Montgomery, J.A., Jr., Stratmann, R.E., Burant, J.C., Dapprich, S., Millam, J.M., Daniels, A.D., Kudin, K.N., Strain, M.C., Farkas, O., Tomasi, J., Barone, V., Cossi, M., Cammi, R., Mennucci, B., Pomelli, C., Adamo, C., Clifford, S., Ochterski, J., Petersson, G.A., Ayala, P.Y., Cui, Q., Morokuma, K., Salvador, P., Dannenberg, J.J., Malick, D. K., Rabuck, A.D., Raghavachari, K., Foresman, J.B., Cioslowski, J., Ortiz, J.V., Baboul, A.G., Stefanov, B.B., Liu, G., Liashenko, A., Piskorz, P., Komaromi, I., Gomperts, R., Martin, R.L., Fox, D.J., Keith, T., Al Laham, M.A., Peng, C.Y., Nanayakkara, A., Challacombe, M., Gill, P.M.W., Johnson, B., Chen, W., Wong, M.W., Andres, J.L., Gonzalez, C., Head Gordon, M., Replogle, E. S., and Pople, J.A. 2003. Gaussian 03, Revision A.1, Gaussian, Inc., Pittsburgh PA. http://www.gaussian.com/index.htm.

Glarborg, P., Kubel, D., Dam Johansen, K., Chiang, H., and Bozzelli, J.W. 1996. Impact of SO_2 and NO on CO oxidation under post flame conditions. *Int. J. Chem. Kinet.*, **28**, 773 790.

Guo, X., Nadykto, A.B., Xu, Y., Zhang, Q., and Hu, J. 2014. Ab *initio* investigation of the thermochemistry and kinetics of the $SO_2 + O_3^- \rightarrow SO_3^- + O_2$ reaction in aircraft engines and the environment. *J. Entropy.*, **16**, 6300 6312.

Hills, A.J., Cicerone, R.J., Calvert, J.G., and Birks, J.W. 1987. Kinetics of the reactions of S_2 with O, O_2, O_3, N_2O, NO, and NO_2. *J. Phys. Chem.*, **91**(5), 1199 1204.

IUPAC. 2006. *Compendium of Chemical Terminology*, 2nd ed. (1997) the "Gold Book", Compiled by A. D. McNaught and A. Wilkinson. Blackwell Scientific Publications, Oxford. Online corrected version: (2006) "transition state theory. https://doi.org/10.1351/goldbook.R05230

Jiang, S. D., Wan, Z. H., Zhou, J. H., Wen, Z. C., and Cen, K. F. 2009. A quantum chemistry study on reaction mechanisms of SO_2 with O_3 and H_2O_2. *J. Zhejiang Univ Sci A.*, **10**(9), 1327 1333.

Louie, D.K. 2005. *Handbook of Sulphuric Acid Manufacturing*, DKL Engineering.

Mayer, P. M.; Parkinson, O. J.; Smith, D. M.; Radom, L. 1998. An assessment of theoretical procedures for the calculation of reliable free radical thermochemistry: a recommended new procedure. *J. Chem. Phys.*, **108**, 604.

Lu, C. W., Wu, Y. J., Lee, Y. P., Zhu, R.S., and Lin, M.C. 2004. Experimental and theoretical investigations of rate coefficients of the reaction S(3P)+O2 in the temperature range 298 878 K. *J. Chem. Phys.*, **121**, 8271.

Merryman, E.M., and Levy, A. 1967. Kinetics of Sulfur Oxide formation in flames: II. Low pressure H_2S flames. *J. Air Pollut. Control Assoc.*, **17**, 800 806.

Montgomery, J.A., Jr., Frisch, M.J., Ochterski, J.W., and Petersson, G.A. 1999. A complete basis set model chemistry. VI. Use of density functional geometries and frequencies. *J. Chem. Phys.*, **110**, 2822.

Montgomery, J.A., Ochterski, J.W., and Petersson, G.A. 1994. A complete basis set model chemistry. VI. Use of density functional geometries and frequencies. *J. Chem. Phys.*, **101**, 5900.

Naidoo, J., Goumri, A., and Paul Marshall, P. 2005. A kinetic study of the reaction of atomic oxygen with SO_2. *Proc. Combust. Inst.*, **30**, 1219.

NIST http://webbook.nist.gov/chemistry/

PEGASUS. 2016. Renewable power generation by solar particle receiver driven sulphur storage cycle. horizon 2020. H2020 LCE 2016 2017. Competitive Low Carbon Energy.

Petersson, G.A., Malick, D.K., and Wilson, W.G. 1998. Calibration and comparison of the Gaussian 2, complete basis set, and density functional methods for computational thermochemistry. *J. Chem. Phys.*, **109**, 10570.

Redfern, P.C., Zapol, P., Curtiss, L.A., and Raghavachari, K. 2000. Assessment of Gaussian 3 and density functional theories for enthalpies of formation of C_1–C_{16} Alkanes. *J. Phys. Chem. A.*, **104**, 5850 5854.

Sebbar, N., Bozzelli, J., Bockhorn, W., and Int, H. 2005b. Enthalpy of formation and bond energies on unsaturated oxygenated hydrocarbons using G3MP2B3 calculation methods. *J. Chem. Kinet.*, **37**, 633 648.

Sebbar, N., Bozzelli, J.W., and Bockhorn, H. 2005a. Thermochemical properties, rotation barriers, and group additivity for unsaturated oxygenated hydrocarbons and radicals resulting from reaction of vinyl and phenyl radical systems with O_2. *J. Phys. Chem. A.*, **109**, 2233 2253.

Sebbar, N., Bozzelli, J.W., and Bockhorn, H. 2014. Thermochemistry and kinetics for 2 Butanone 1 yl Radical $(CH_2{\cdot}C({=}O)CH_2CH_3)$ Reactions with O_2. *J. Phys. Chem. A.*, **118**, 21–37.

Tsuchiya, K., Kamiya, K., and Matsui, H. 1997. Studies on the oxidation mechanism of H_2S based on direct examination of the key reactions. *Int. J. Chem. Kinet.*, **29**, 57 66.

Wong, M.W., and Radom, L. 1998. Radical addition to alkenes: further assessment of theoretical procedures. *J. Phys. Chem. A.*, **102**, 2237 2245.

Yilmaz, A., Hindiyarti, L., Jensen, A.D., Glarborg, P., and Marshall, P. 2006. Thermal dissociation of SO_3 at 1000 1400 K. *J. Phys. Chem. A.*, **110**, 6654 6659.

Zhang, Y., Yang, H., Zhou, J., Wang, Z., Liu, J., and Cen, K. 2014. Detailed kinetic modeling of homogeneous H2SO4 decomposition in the sulfur iodine cycle for hydrogen production. *Applied Energy.*, **130**, 396 402.

Zhao, Y., Lynch, B.J., and Truhlar, D.G. 2004. Quantum chemical study of C SH bond dissociation energies for some thiol compounds. *J. Phys. Chem. A.*, **108**, 2715.

Sebbar, N.; Bozzelli, J. W.; Bockhorn, H.; Trimis, D.
A thermochemical study on the primary oxidation of sulfur.
2019. Combustion science and technology, 191.
doi: 10.5445/IR/1000086449

Sebbar, N.; Bozzelli, J. W.; Bockhorn, H.; Trimis, D.
A thermochemical study on the primary oxidation of sulfur.
2019. Combustion science and technology, 191 (1), 163–177.
doi:10.1080/00102202.2018.1455134